



## Breakdown-induced negative charge in ultrathin SiO<sub>2</sub> films measured by atomic force microscopy

M. Porti, M. Nafra, M. C. Blüm, X. Aymerich, and S. Sadewasser

Citation: [Applied Physics Letters](#) **81**, 3615 (2002); doi: 10.1063/1.1519357

View online: <http://dx.doi.org/10.1063/1.1519357>

View Table of Contents: <http://scitation.aip.org/content/aip/journal/apl/81/19?ver=pdfcov>

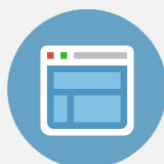
Published by the [AIP Publishing](#)

---



## Re-register for Table of Content Alerts

Create a profile.



Sign up today!



## Breakdown-induced negative charge in ultrathin SiO<sub>2</sub> films measured by atomic force microscopy

M. Porti,<sup>a)</sup> M. Nafria, M. C. Blüm,<sup>b)</sup> and X. Aymerich

*Departament d'Enginyeria Electrònica, Universitat Autònoma de Barcelona, ETSE, Edifici Q, 08193 Bellaterra, Barcelona, Spain*

S. Sadewasser

*Hahn-Meitner-Institut, Glienicker Str. 100, 14109 Berlin, Germany*

(Received 10 July 2002; accepted 16 September 2002)

Atomic-force-microscopy-based techniques have been used to investigate at a nanometer scale the dielectric breakdown (BD) of ultrathin (<6 nm) SiO<sub>2</sub> films of metal-oxide-semiconductor devices. The results show that BD leads to negative charge at the BD location and the amount of created charge has been estimated. Moreover, the comparison of the charge magnitude generated during current-limited stresses and stresses without current limit demonstrates that the observed BD induced negative charge is related to the structural damage created by the oxide BD. © 2002 American Institute of Physics. [DOI: 10.1063/1.1519357]

Although much work has been dedicated to the study of the dielectric breakdown (BD) of SiO<sub>2</sub> films in metal-oxide-semiconductor (MOS) devices, due to its importance for the reliability of microelectronic technologies, a definitive picture for the mechanism which finally causes the oxide failure is still missing. However, it is accepted that BD is (i) the consequence of a previous degradation stage during which defects are generated in the oxide<sup>1</sup> and (ii) an extremely local phenomenon which takes place in areas of the order of  $10^{-13}$ – $10^{-12}$  cm<sup>2</sup> (=10–100 nm<sup>2</sup>).<sup>2</sup> The last property points out the suitability of scanning probe microscopy techniques to characterize the BD event, since their large lateral resolution allows the study of areas in the nanometer range. In particular, the conductive atomic force microscope (C-AFM), which allows the simultaneous collection of topographical and electrical (current) information,<sup>3–5</sup> has recently been used to study the degradation and breakdown of ultrathin gate oxides. The analysis of the electrical conduction properties of nanometric oxide areas, before and after BD, provided direct experimental evidence of the local nature of the degradation and breakdown mechanisms.<sup>4</sup> Moreover, it showed that BD, although triggered at one point, electrically propagates to neighbor areas.<sup>5</sup> In the present work, we will show that BD leads to the creation of negative charge in the oxide, which is closely related to the microscopic damage induced.

The polysilicon electrode of MOS structures (4.2- and 5.9-nm-thick oxides thermally grown on a *n*-doped Si substrate) was removed to locally stress the bare oxide with the tip of the atomic force microscope (AFM). Therefore, in this setup, the conductive tip plays the role of the metal electrode of a MOS structure, which has been experimentally determined to have typical areas of ≈300–1000 nm<sup>2</sup> (depending on the tip).<sup>4</sup> Ramped voltage stresses (RVS) or constant voltage stresses were used to induce the oxide BD. The current

was sometimes limited to 10 or 100 pA (current limited stresses). After the electrical stress, the broken down locations have been imaged with: a C-AFM (contact mode) and/or an AFM working in noncontact mode that, when required, is able to operate as a Kelvin probe force microscope (KPFM), which measures the contact potential difference (CPD) of the structure.<sup>6</sup> With these setups, topography, current (when a constant voltage is applied between the tip and the sample), and/or CPD images were measured to analyze the effect of the BD event.

Figure 1 shows (a) the topography and (b) the current images taken during a C-AFM measurement on an oxide region that contains a BD spot. Larger currents are measured at the BD spot, as expected. Moreover, the BD event has induced a hillock in topography, suggesting some morphological damage of the oxide. However, it can be shown that the characteristics of the topography features depend on the measurement conditions: operation mode, applied voltage, and cantilever spring constant.<sup>7</sup> As an example, Figs. 1(c) and 1(d) show the topography measured at the same BD location with the AFM operated in noncontact mode, when two different voltages were applied to the structure. Depending on the applied voltage, either hillocks or depressions are observed. Now, depressions are measured, whose depth depends on the applied voltage. When the AFM is operated in Kelvin mode (KPFM), some topographical structure is observed [Fig. 1(e)]. Due to the long range electrostatic forces, the measured CPD is an averaged quantity. However, the determination of the topography relies on the short range force gradient, thus, some residual topographical signal is observed. Considering all these results, we can conclude that the topography observations are *not real* changes of the oxide morphology but artifacts of the measurement technique. In this sense, it is worth emphasizing that the CPD is smaller at the BD spot [Fig. 1(f)]. This result clearly indicates that some negative charge has been induced at the BD location. The topographical features observed have been pointed out to be the consequence of the electrostatic interactions between this negative charge and the conductive tip.<sup>7</sup>

<sup>a)</sup>Electronic mail: marc.porti@uab.es

<sup>b)</sup>Currently with: Institut de Physique de la Matière Condensée, Université de Lausanne, 1015 Lausanne, Switzerland.

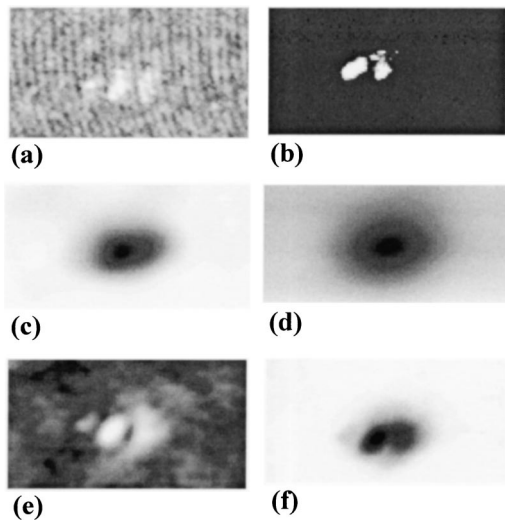


FIG. 1. BD of a 4.2 nm oxide is induced during a RVS using the tip of the microscope as the metal electrode of a MOS structure. The oxide is imaged afterwards. (a) Topography and (b) current images measured with the C-AFM (contact mode). Apart from the expected current increment (1.4 nA), the BD has led to a hillock in topography (1.2 nm high); (c) and (d) correspond to the topography of the same spot measured with the AFM operated in noncontact mode, when +1V and -1V were applied to the sample, respectively. Depressions are now measured, whose depth depends on the applied voltage [14 nm in (c) and 8 nm in (d)]. (e) Topography image of the same spot taken with the AFM operated as KPFM. A hillock is again observed. The corresponding CPD is shown in (f). The CPD is 0.4 V smaller at the BD location, suggesting the presence of negative charge. The topography features (a), (c), (d), and (e) are the consequence of electrostatic interactions between this charge and the conductive tip. The size of all images is  $0.5 \times 0.25 \mu\text{m}^2$ .

Negative charge in the oxide after BD has already been reported, from indirect electrical measurements on MOS field effect transistors.<sup>8</sup> However, the present results, in particular the CPD image, provide a direct demonstration of the creation of this charge. Moreover, they allow us to determine the amount of BD induced negative charge. First, it can be determined from the CPD image [Fig. 1(f)]. Assuming that the tip-sample system is roughly a parallel-plate capacitor<sup>9</sup> (an approximation that will lead to charge values smaller than the actual ones),<sup>9</sup> the charge per unit area ( $Q'$ ) can be calculated from  $Q' = \Delta V C'_{\text{ox}}$ , where  $C'_{\text{ox}} = 8.2 \times 10^{-7} \text{ F/cm}^2$  is the capacitance of the oxide layer for the 4.2 nm oxide (we have neglected the series capacitance corresponding to the vacuum gap when working in noncontact, which would lead to a smaller  $C'_{\text{ox}}$ ). To roughly estimate this charge, we have considered that  $\Delta V$  corresponds to the maximum CPD, so that it will be actually underestimated. This calculation leads to a charge density of  $\sim 0.3 \mu\text{C/cm}^2 \sim 2 \times 10^{12} \text{ e/cm}^2$ , in agreement with the values of the trapped charge density at BD measured during conventional electrical tests, and that has been related to the critical density of generated defects needed to trigger BD.<sup>10,11</sup> If we further assume a uniform charge distribution in an area of  $\sim 10^3 \text{ nm}^2$  (a very conservative value of the MOS structure area), this charge corresponds to  $\sim 20$  electrons in the BD spot. Second, we have determined the amount of negative charge from the C-AFM topography images, since the observed features are a consequence of this charge (we have chosen the C-AFM images because this technique simultaneously collects the current through the oxide, an extensively

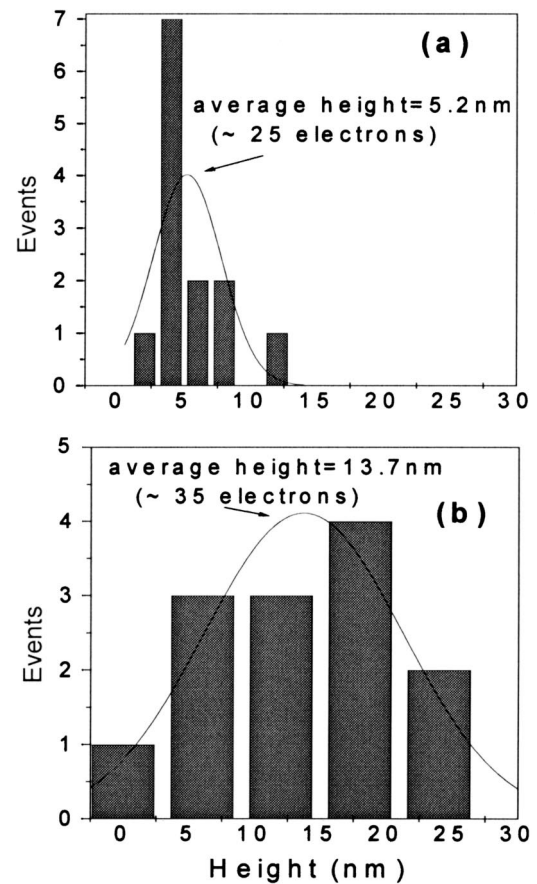


FIG. 2. Distributions of heights of the topographical features measured at different BD locations with the C-AFM. BD was induced during (a) current limited stresses (CLS) and (b) nonlimited current stresses. Best fit curves have been plotted as a visual aid. The average heights and standard deviations are (a)  $5.2 \pm 2.6 \text{ nm}$  and (b)  $13.7 \pm 7.6 \text{ nm}$ . From electrostatic considerations, these heights would be associated with approx. 25 and 35 BD induced negative charges, respectively.

used monitor of oxide degradation and BD). To determine the magnitude of this charge from these images, we have assumed that the additional deflection force that the cantilever is experiencing due to the presence of this charge (given by Hooke's law) equals the electrostatic force between the tip and the negative charge. Moreover, we have considered that the charge that leads to this deflection is concentrated at the point of maximum height of the spot, at the  $\text{SiO}_2/\text{Si}$  interface. With these assumptions, a charge of  $\sim 30$  electrons has been obtained for the BD spot shown in Fig. 1 (1.2 nm high). Note that, despite the simplistic assumptions considered for these computations, the charge amount obtained from CPD and C-AFM topography images are very close. Therefore, the topography heights of the BD spots can be used to get rough estimations of the amount of negative charge induced by the BD event, which will be specially suited for comparison purposes.

The negative charge present in the oxide after the BD event must be intimately related to the microscopic physics of the BD process and, consequently, to trap generation. Trap generation during electrical stress involves physical changes in the oxide structure associated with bulk oxide bond breakage and rearrangement. In this sense, neutral  $E'$  centers, which have been shown to be generated in oxides subjected to electrical stress,<sup>12</sup> have been recently pointed out as prob-

able candidates for the defect centers inducing electrical degradation and BD of the stressed oxide films.<sup>13,14</sup> We can, therefore, speculate that electron trapping in these centers could be the origin of the negative charge observed. Although further work is required to determine the actual nature of this charge (which is out of the scope of this letter), it can be demonstrated that it is correlated to the microscopic damage induced by the BD event. To establish this relation, different oxide locations have been broken down with the C-AFM during current limited stresses (CLS) and stresses without current limitation. Topography and current images of the BD spots have been taken afterwards. In the current images, CLS tests induce BD spots with smaller areas, since these tests avoid the complete development of the BD path and are, therefore, “softer” than nonlimited current stresses.<sup>5,15</sup> Moreover, hillocks were measured in the topographical images. The distribution of heights of these hillocks has been plotted for the case of CLS [Fig. 2(a)] and stresses without current limit [Fig. 2(b)]. Note that, despite the dispersion of results, which can be attributed to the intrinsic randomness of the BD phenomenon,<sup>5</sup> there is a correlation between the BD hardness and the height of the hillocks measured with the C-AFM: the larger the hardness (nonlimited case), the larger the height of the hillocks. We have shown above that the heights are related to the BD induced charge. Thus, we can conclude that the amount of charges is smaller for CLS, corresponding to a smaller amount of defects involved in the BD process in this case, as expected.<sup>5</sup>

In summary, CPD images show that the BD event induces negative charge in the oxide. The amount of charge has been roughly estimated from the CPD image and from the heights of the hillocks measured in the C-AFM topography images. Negative charge densities of  $\sim 2 \times 10^{12}$  e/cm<sup>2</sup> have been measured. Although further work is needed to determine the microscopic nature of this charge, its relation with the structural damage induced by the BD event has been demonstrated through the comparison of the amount of

charge induced during CLS and nonlimited stresses.

The authors thank G. Bersuker and P. M. Lenahan for helpful discussions. This work has been partially supported by the Dirección General de Investigación Científica del MCyT (project No. BFM2000-0343) and Nanofab (Contract No. ERBFMRXCT970129) of the TMR program of EC.

- <sup>1</sup>D. J. DiMaria, E. Cartier, and D. Arnold, *J. Appl. Phys.* **73**, 3367 (1993).
- <sup>2</sup>J. Suñé and E. Miranda, in *The Physics and Chemistry of SiO<sub>2</sub> and the Si-SiO<sub>2</sub> Interface-4*, edited by H. Z. Massoud, I. J. R. Baumvol, M. Hirose, and E. H. Poindexter (The Electrochemical Society, Pennington, NJ, 2000), Vol. 4, pp. 333–344.
- <sup>3</sup>A. Olbrich, B. Ebersberger, and C. Boit, *Appl. Phys. Lett.* **73**, 3114 (1998).
- <sup>4</sup>M. Porti, M. Nafria, X. Aymerich, A. Olbrich, and B. Ebersberger, *J. Appl. Phys.* **91**, 2071 (2002).
- <sup>5</sup>M. Porti, M. C. Blüm, M. Nafria, and X. Aymerich, *40th Annual IEEE International Reliability Physics Symposium Proceedings* (IEEE, New York, 2002).
- <sup>6</sup>Ch. Sommerhalter, Th. Glatzel, Th. W. Matthes, A. Jäger-Waldau, and M. Ch. Lux-Steiner, *Appl. Surf. Sci.* **157**, 263 (2000).
- <sup>7</sup>M. Porti, M. Nafria, M. C. Blüm, X. Aymerich, and S. Sadewasser, to be presented at 7th International Conference on Nanometer-Scale Science and Technology and 21st European Conference on Surface Science, 2002.
- <sup>8</sup>T. Pompl, H. Wurzer, M. Kerber, R. C. W. Wilkins, and I. Eisele, *37th Annual IEEE International Reliability Physics Symposium Proceedings, 23–25 March 1999, San Diego, CA* (IEEE, New York, 1999), p. 82.
- <sup>9</sup>J. W. Hong, S. M. Shin, C. J. Kang, Y. Kuk, and Z. G. Khim, *Appl. Phys. Lett.* **75**, 1760 (1999).
- <sup>10</sup>D. J. Dumin, J. R. Maddux, R. S. Scott, and R. Subramoniam, *IEEE Trans. Electron Devices* **41**, 1570 (1994).
- <sup>11</sup>R. Rodríguez, M. Nafria, J. Suñé, and X. Aymerich, *IEEE Trans. Electron Devices* **45**, 881 (1998).
- <sup>12</sup>P. M. Lenahan, J. J. Mele, R. K. Lowry, and D. Woodbury, *J. Non-Cryst. Solids* **266**, 835 (2000).
- <sup>13</sup>P. M. Lenahan, J. J. Mele, J. P. Campbell, A. Y. Kang, R. K. Lowry, D. Woodbury, S. T. Liu, and R. Weimer, *39th Annual IEEE International Reliability Physics Symposium Proceedings, 30 April – 3 May 2001, Orlando, FL* (IEEE, New York, 2001), p. 150.
- <sup>14</sup>G. Bersuker, A. Korin, Y. Jeon, and H. R. Huff, *Appl. Phys. Lett.* **80**, 832 (2002).
- <sup>15</sup>B. P. Linder, J. H. Stathis, R. A. Wachnik, E. Wu, S. A. Cohen, A. Ray, and A. Vayshenker, *IEEE Symposium on VLSI Technology* (IEEE, New York, 2000), pp. 214–215.